Particulate Rare Earth Element behavior in the North Atlantic (GEOVIDE cruise): supplementary material

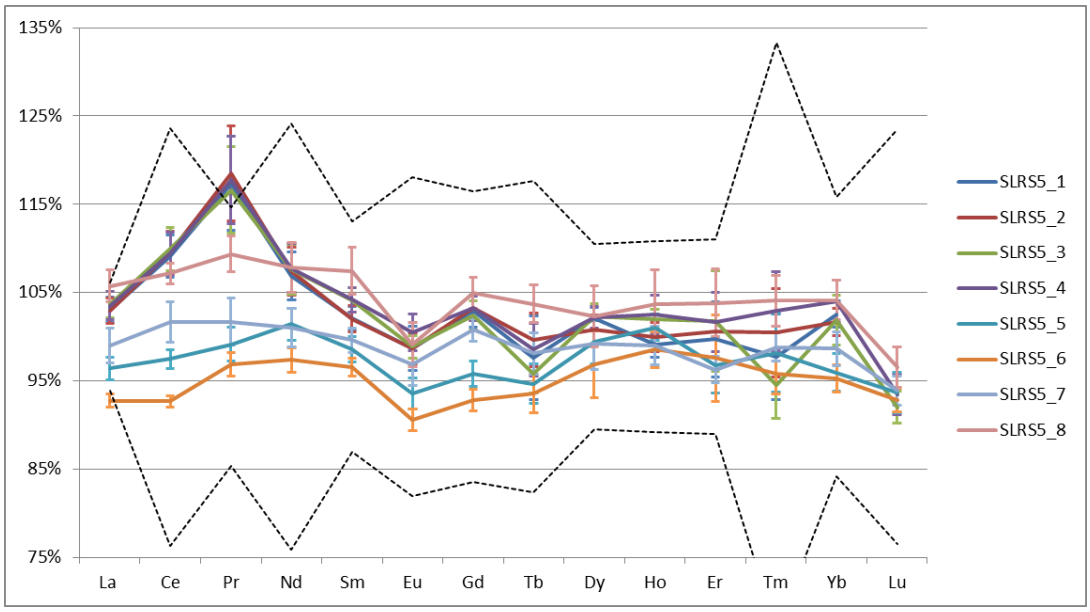

Figure S1: Percentage of recovery of the CRM SLRS-5 analyzed concomitantly with the samples of the study. The dotted lines bracket the consensual range from (Yeghicheyan et al., 2013).

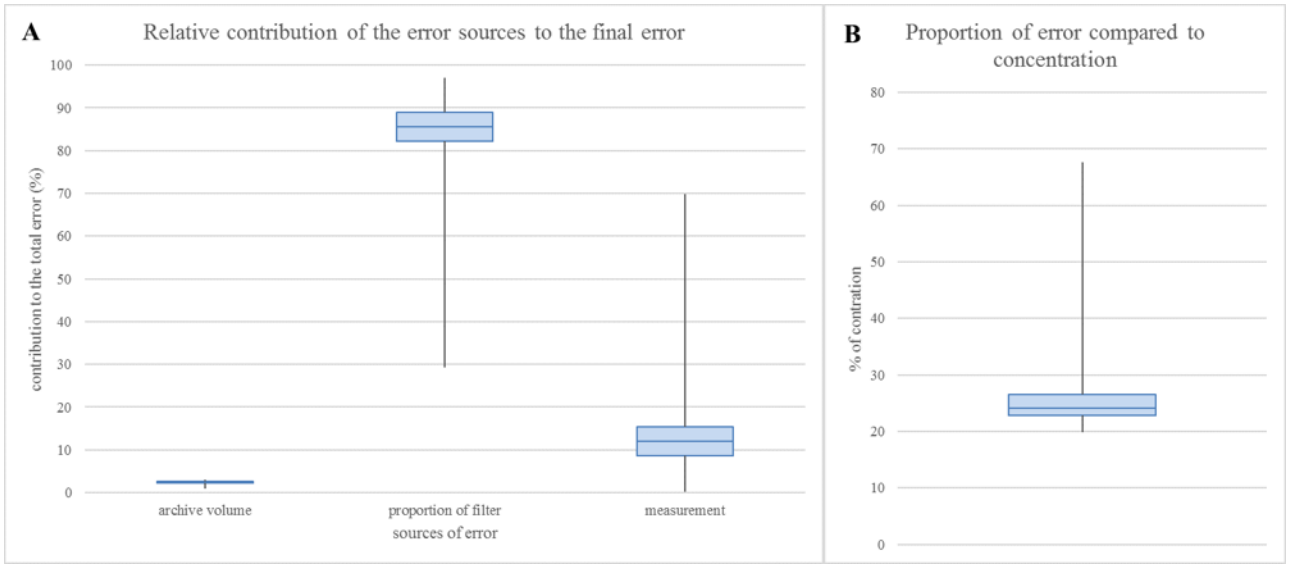

Figure S2: A. boxplots of the relative contribution to the most important sources of error to the total error and B. boxplot of the proportion of error compared to concentration. It takes in account all the REEs, in all the samples.

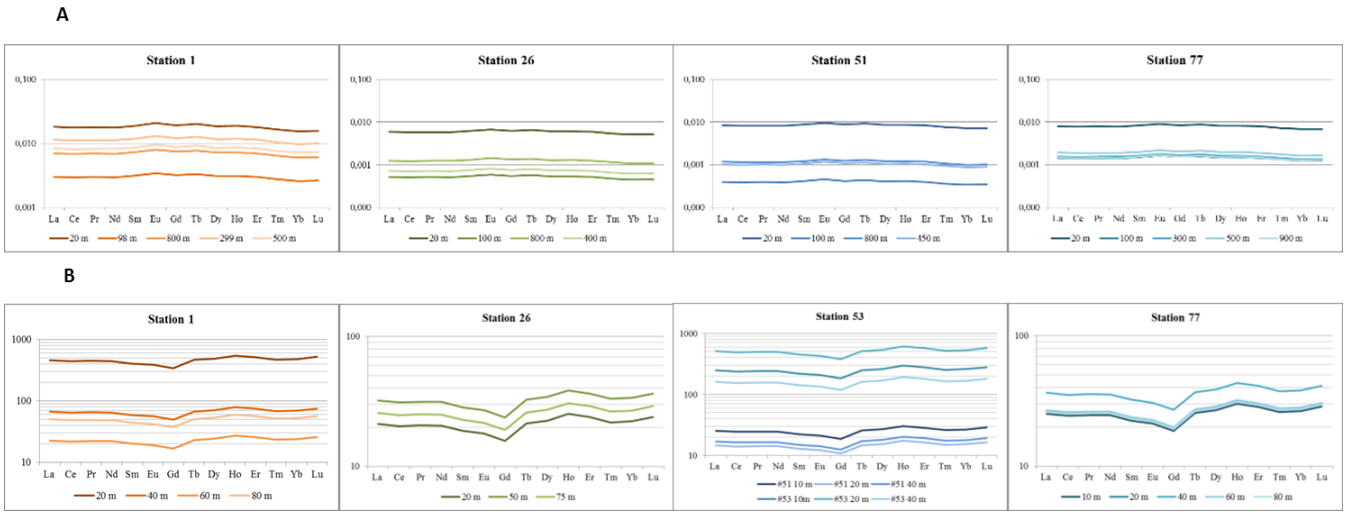

Figure S3: Lithogenic fractions at stations #1, #26, #51, #53 and #77, determined from particulate ^{232}Th concentrations and normalized to A. PAAS, from surface to deep depths, and B. Northeast Atlantic aerosol (Patey et al., 2015), for the surface layer.

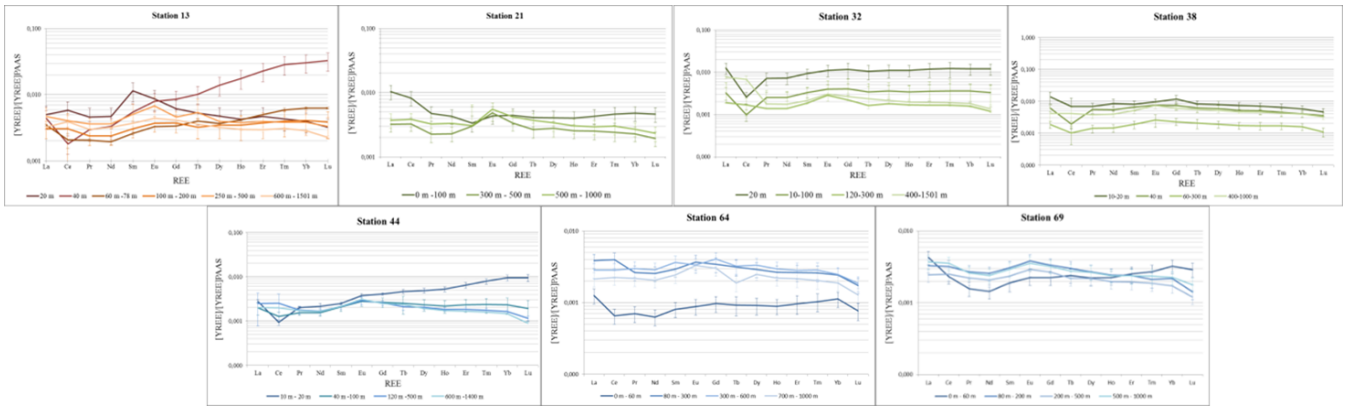

Figure S4: PAAS-normalized REE patterns of the total fraction, averaged by depth layers, at stations #13, #21, #32, #38, #44, #64 and #69.

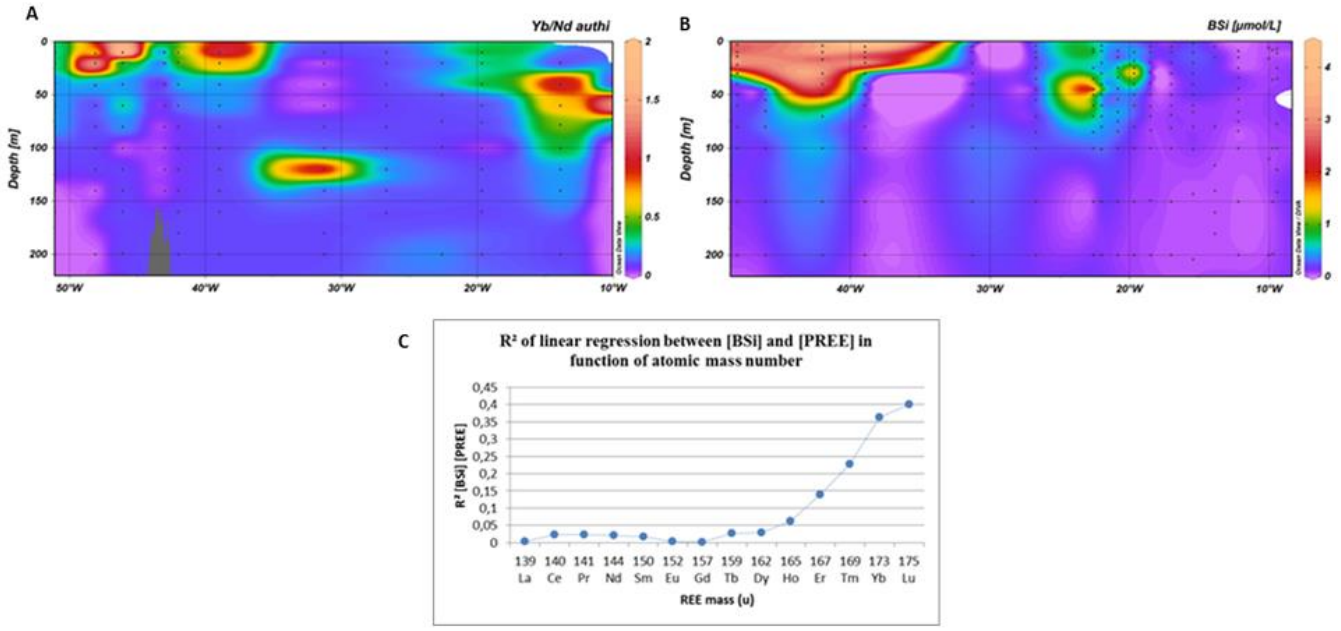

Figure S5: PAAS-normalized REE patterns of the total fraction, averaged by depth layers, at stations #13, #21, #32, #38, #44, #64 and #69.

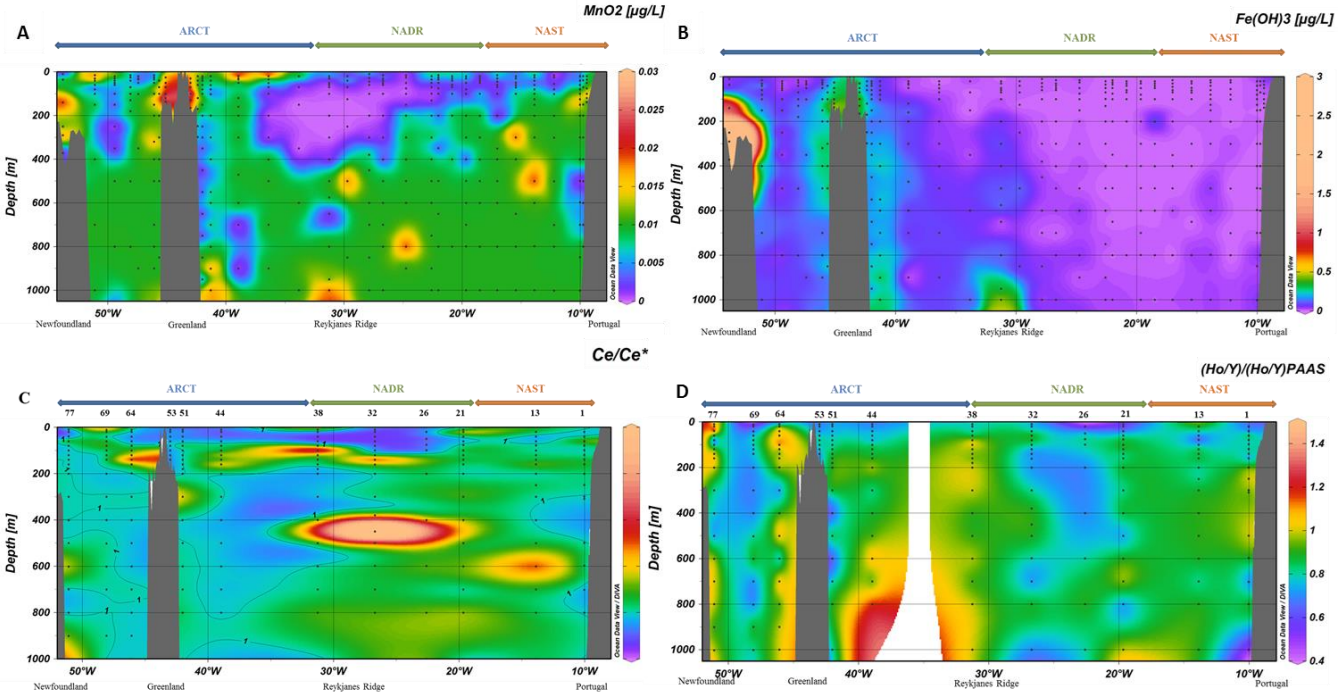

Figure S6: A. MnO_2 and B. $Fe(OH)_3$ concentrations (in µg.L^{-1}) calculated with the formula proposed by Lam et al. (2017) using particulate Mn, Fe and Al concentrations from Gourain et al. (2019). C. Ce anomaly Ce/Ce* and D. particulate PAAS-normalized Ho/Y ratio. Data are interpolated with the DIVA gridding function of Ocean Data View along the section.